Brain Research, 437 (1987) 264–282
Elsevier

BRE 13158

Ultrastructural localization of β-adrenergic receptor-like immunoreactivity in the cortex and neostriatum of rat brain

Chiye Aoki[1], Tong H. Joh[2] and Virginia M. Pickel[1]

Divisions of [1]Neurobiology and [2]Molecular Neurobiology, Department of Neurology, Cornell University Medical College, New York, NY 10021 (U.S.A.)

(Accepted 9 June 1987)

Key words: β-Adrenergic receptor; Neostriatum; Synaptosome; Somatosensory cortex; Anterior cingulate cortex; Postsynaptic density; Membrane recycling

We sought to quantitatively examine the processes containing β-adrenergic receptor-like immunoreactivity (β-AR-LI) in the cerebral cortex and neostriatum using a previously characterized rabbit antiserum to frog erythrocyte β-ARs under optimized immunolabeling conditions. Quantitative assessments of the laminar distribution of β-AR-LI in the cortex was achieved by computer-assisted image analysis of immunoautoradiographs and by quantitative electron microscopic analysis of peroxidase–antiperoxidase (PAP) labeling in aldehyde-fixed sections and unfixed synaptosomes. In the somatosensory and anterior cingulate cortical areas, light microscopy of aldehyde-fixed sections immunolabeled by the PAP method revealed small (0.5–1.0 μm) punctate processes in all layers. In the deeper layers, rims of immunoreactivity around the plasmalemma of a population of neuronal perikarya and processes were also observed. By immunoautoradiography, labeling was seen in distinct, laminar distributions resembling the reported autoradiographic patterns using radioligands[34,40,46]. By electron microscopy, the immunoreactive profiles in all cortical layers were primarily thick and thin postsynaptic densities (PSDs), comprising 4% of all identifiable PSDs in fixed sections and 12% in unfixed synaptosomal preparations. Also labeled were saccules of smooth endoplasmic reticulum and pinocytotic vesicles in dendrites, glial processes and lightly myelinated axons. In the neostriatum, the density of autoradiographic immunoreactivity was equivalent to the heavily labeled laminae of the cerebral cortex. Immunoreactivity detectable by light microscopy included punctate processes and rims of perikarya, as was seen in the cerebral cortex. The PAP reaction was shown by electron microscopy to be localized to the cytoplasmic surface of plasmalemma of a few proximal dendrites, but was most prominently associated with PSDs of dendritic spines. Preadsorption of the antiserum with a partially purified β-AR preparation abolished all detectable immunoreactivity. These results provide further support for the specificity of the antiserum for β-ARs, and are the first quantitative ultrastructural evidence for association of β-AR-LI with PSDs in the cerebral cortex. The neostriatum, whose major catecholaminergic innervation is dopaminergic, and not noradrenergic, is also confirmed to exhibit high levels of β-AR-LI within subcellular structures analogous to those seen in the cerebral cortex. The ultrastructural distribution of β-AR-LI in the two regions provides morphological support for the receptor's membrane-associated recycling, axonal transport, function at both excitatory and inhibitory synapses, and role in interactions between specific neurons and glia.

INTRODUCTION

The macroscopic distribution of β-adrenergic receptors (β-ARs) in the CNS has been visualized by detection of specific binding of radioligands within frozen sections[1,11,34,40,46]. However, these radioligands do not remain stably bound during the processes required for light and electron microscopy. Furthermore, even with more stable binding, such as in the photoaffinity-labeling method that generates covalent bonds between radioligands and receptors[29], statistical analysis of individual silver grains would be necessary to determine the pre- or postsynaptic localization of binding sites[20]. An earlier light and electron microscopic study using peroxidase–antiperoxidase (PAP)-immunocytochemistry with a polyclonal antiserum against the β_2-adrenergic receptor from frog erythrocytes has shown that the peroxidase reaction product is associated with postsynaptic densities (PSDs) and also generally distributed throughout the perikarya and dendrites of selective neurons within several regions of the amphibian and

Correspondence: C. Aoki, Division of Neurobiology, Department of Neurology, Cornell University Medical College, 411 E. 69th St., New York, NY 10021, U.S.A.

0006-8993/87/$03.50 © 1987 Elsevier Science Publishers B.V. (Biomedical Division)

rat brain[54]. We have now undertaken a more critical, detailed evaluation of the regional and subcellular localization of the antigenic sites recognized by this antiserum. Two brain regions, the neostriatum and the cerebral cortex, recognized to contain high densities of β-AR[34,40,46] but very different degrees of noradrenergic innervations[16,35,36], were chosen for this study. We specifically sought: (1) to determine whether a more selective subcellular localization could be achieved using optimized (a) fixation, (b) penetration-enhancement methods, and (c) a range of dilutions of the primary antiserum in sections of the striatum and cortex and in unfixed cortical synaptosomal preparations; then (2) to quantitatively determine whether the antiserum recognized sites having a macroscopic distribution similar to that of radioactive ligands; and (3) to quantitatively assess the ultrastructural distribution of antigenic sites.

MATERIALS AND METHODS

Source of the antibodies

A polyclonal antiserum was raised in rabbits, using β_2-adrenergic receptors purified from frog erythrocyte membranes by Dr. C.D. Strader (Merck, Sharp and Dohme Research Laboratories)[54]. Iodinated donkey anti-rabbit IgG (^{125}I-IgG) was purchased from Amersham and goat anti-rabbit IgG was purchased from Miles Laboratory (Elkhart). Rabbit PAP was prepared and generously provided by Corinne Abate, Laboratory of Molecular Neurobiology, Cornell University Medical College.

Fixation conditions and penetration enhancing methods

Optimal fixation conditions were determined by comparing the detected immunoreactivity in sections from the brains of 47 adult rats receiving aortic arch perfusions with either 3.75% acrolein/2% paraformaldehyde or with 0.1% glutaraldehyde/4% paraformaldehyde in 0.1 M phosphate buffer (PB) at pH 7.4. The animals were deeply anesthetized (50 mg/kg Nembutal, i.p.) and perfused through the aortic arch for 6 min with either cold (10 °C) or warm (32 °C) fixative. The brains were removed at the termination of the perfusion, and 2 mm coronal wedges were postfixed in the same solutions for 30 or 60 min at the corresponding cold or warm temperatures. Sections ranging in thickness from 30 to 40 μm were prepared with a Vibratome. The acrolein-fixed sections then were immersed in 1% sodium borohydride in PB for 30 min to terminate acrolein's cross-linking activity[49], then rinsed twice in PB. This step was omitted for tissues fixed with glutaraldehyde/paraformaldehyde, since it was previously shown not to be necessary[45].

Methods tested for the possible enhancement of penetration of antisera included rapid freeze-thawing of tissues cryoprotected with 30% sucrose, 30 min pretreatment of Vibratome sections with 0.2% of the detergents, Triton X-100, saponin and digitonin[17], and pretreatment with graded concentrations (0–40%) of ethanol in PB over 15-min total periods.

Unfixed synaptosomal preparations

Synaptosomal fractions from fresh dog cerebral cortex were used to characterize the binding of the β-AR-antiserum to unfixed tissue. These were prepared[7] and generously provided by the laboratory of Dr. Philip Siekevitz (Rockefeller University). The synaptosomal fractions were suspended in 0.32 M sucrose/0.1 M $NaHCO_3$, pH 7.4 and stored on ice until the beginning of the period of incubation with the antiserum.

Labeling procedure

The modified procedure for PAP-immunocytochemical labeling[52] of Vibratome sections has already been described in detail[45]. The methods for labeling unfixed synaptosomes were developed in this study.

Aldehyde-fixed sections were washed through two changes of 0.1 M Tris (pH 7.6)/0.9% NaCl (TS) containing 3% goat serum (GS), then incubated for periods of 1–3 days at room temperature or at 10 °C with the β-AR-antiserum diluted at either 1:100, 1:500, 1:1000, 1:2000 or 1:4000 using 1% GS/TS. The sections were subsequently washed, incubated with goat anti-rabbit immonoglobulin (IgG) and PAP which was visualized using diaminobenzidine as the chromogen (see below).

Unfixed synaptosomal fractions were similarly washed through two changes of TS, then incubated with 1:50, 1:100, 1:300 or 1:1000 dilutions of the antiserum for 2–8 h. Following the incubation with the primary antiserum, the samples were rinsed twice at 15-min intervals with 1% GS/TS, then incubated with

a 1:50 dilution of goat anti-rabbit IgG fraction in 1% GS/TS for 1 h. This was followed by two 15-min rinses with 1% GS/TS, a 1-h incubation with a 1:100 dilution of rabbit PAP, and 15-min rinses with TS. The samples finally were reacted with 3,3'-diaminobenzidine and hydrogen peroxide[52]. All incubations were at room temperature and the preparations were gently agitated on a rotating disk. The incubation media of synaptosomal fractions were changed by removing the supernatants of 700 $g \times 0.5$-min centrifugations, then resuspending the pellet in the next medium by vortexing. The 10 cycles of incubation–centrifugation–vortexing totalled approximately 14 h.

Intensification of reaction

In some cases, the immunocytochemical reaction product was intensified by double-bridging the PAP product[21]. This latter intensification was achieved by passing tissues through two complete cycles of incubations with goat anti-rabbit IgG/PAP following a single, overnight incubation with the primary antiserum[39].

Microscopic examination

For light microscopy, immunocytochemically labeled sections were mounted on gelatin-coated glass slides and examined with bright-field or Nomarski optics. For electron microscopy, the labeled sections and synaptosomal pellets were fixed with 1% glutaraldehyde for 10 min at room temperature, then with 2% OsO_4 in 0.1 M PB and dehydrated. Subsequently, the thick sections were flat-embedded in Epon 812 and the anatomically identified regions from these sections were re-embedded in capsules. Synaptosomal pellets were embedded in Epon that was directly poured into centrifuge tubes. Application of vacuum was necessary for efficient infiltration of Epon into the pellets. Ultrathin sections from the extreme outer surface of the Vibratome sections and from various depths through synaptosomal pellets were collected, counterstained with uranyl acetate and lead citrate, and examined with a Philips 201 electron microscope.

Radiochemical identification of the antigenic sites in sections and synaptosomal pellets

A radioimmunohistochemical method developed by McLean et al.[31] was used for rapid and quantitative assessment of the antigenic sites in sections. After two rinses with 1% GS/TS to remove the unbound antibody, sections were incubated with a 1:50 dilution of donkey anti-rabbit ^{125}I-IgG in 1% GS/TS for a period ranging from 30 min up to 2 h at room temperature. Sections were processed through repeated changes of TS until negligible amounts of radioactivity were detected in the wash. They were then mounted on acid-washed slides freshly coated with 0.25% gelatin/0.025% chromium potassium sulfate. The dry, mounted sections were placed in direct contact with tritium-sensitive LKB Ultrofilm for 12–48 h, then developed for 3 min in GBX. These films, which were devoid of artifacts associated with uneven spreading of liquid emulsion, were used for computer-assisted densitometric analyses (see below). For more detailed light microscopic examination, the slides were dipped in Ilford-L4 emulsion diluted 1:1 with water at 50 °C, exposed in light-proof boxes at 4 °C for 4–21 days and developed for 2 min at 17 °C with D-19. Synaptosomal pellets were similarly incubated with the primary antiserum and ^{125}I-IgG, then rinsed repeatedly over a period of 2 h and counted in scintillation counters. Background labeling of synaptosomes was assessed from scintillation counts that resulted from omitting the incubation in the primary antiserum.

Macroscopic analysis of immunoautoradiographs

Immunoautoradiographic images of LKB Ultrofilms, developed after 0.5–2 days of exposure, were digitized by a semi-automated image analysis system (Eyecom II and a Microvax computer)[22]. Within each anatomical area of the digitized image of coronal sections, repeated measurements of relative optical densities (R.O.D.) were taken. The R.O.D. was standardized for every section by relating to a gray scale (Kodak) superimposed on the film. These R.O.D. values had subtracted from them the background O.D. generated by fluctuations in the light transmission to and electronically within the TV monitor as well as O.D. of non-tissue areas of the film. The mean and standard deviations of R.O.D. values within each area were normalized to the mean value of the supragranular layer of the somatosensory cortex in sections of forebrain, and to the mean value of the molecular layer of cerebellum in the caudal sections. For the analysis of antigenic sites within

the cortex and neostriatum, these R.O.D. values were, in turn, used to calculate the mean of normalized R.O.D. values: (1) for each of the 5 animals; and (2) across the 5 animals. Student's *t*-test was performed to the values of (2) to calculate the greatest error values with 90–99.5% certainties. Representative values obtained from the cerebellum and cerebral cortex/neostriatum are given in Fig. 1 and Table II, respectively.

Semiquantitative ultrastructural analysis of the distribution of the immunolabeled processes

Care was taken to prepare trapezoids of Epon blocks whose parallel edges spanned the entire thickness of the cortex. The shorter unparallel edges, therefore, marked the pial and corpus callosal limits of the cortex. Ultrathin sections spanning from the most superficial (almost all Epon) to deeper (almost all tissue) parts of blocks were serially collected. Within these sections, the square areas bounded by grid mesh containing Epon–tissue interface were selected for quantitative ultrastructural analyses. Using grid mesh as tick marks of an internal scale, the position of each chosen square area relative to the pial and callosal edges of trapezoids was determined and converted to laminar depth position. Within chosen squares, tissue (or Epon) areas were determined by measuring their proportionality to the whole square area, the latter of which was always 5100 μm^2. This proportionality, in turn, was determined with the aid of calibration marks within the electron microscope screen. All immunoreactive elements within the tissue-area of chosen squares were photographed at a magnification of 15,000×. These electron micrographs were used to tally the immunoreactive elements categorized as the following: synaptic terminal (identified by the presence of clusters of vesicles), dendritic process (identified by the presence of postsynaptic densities), myelinated axon, or small-calibre (less then 0.2 μm diameter) unidentifiable process. In addition, two or more immunoreactive processes residing side-by-side were also tallied. These values are represented in Table I. For the analysis of laminar distribution of β-AR-LI, the numbers of immunoreactive processes were determined within each laminar position, and the frequencies of detection corrected for the differences in total surveyed areas. The values are represented as bar graphs in Fig. 6.

RESULTS

Identity of immunoreactive material

Immunoautoradiographs of the cerebellum on LKB Ultrofilm were examined for the initial, rapid, macroscopic assessments of the antiserum's specificity for β-ARs. Computer-assisted image analysis revealed relative optical density values reflecting immunoreactivity in the molecular layer that was 2–3-fold higher than that of the Purkinje-granular layer and the white matter under various conditions. The methodological variables included the dilutions of primary antiserum, fixations and penetration enhancements. An example of the analyzed immunoautoradiographs and relative optical density values is given in Fig. 1.

Using this antiserum, the initial discrimination of specific vs non-specific immunolabeling in the cerebral cortex and the neostriatum was based on examinations of PAP-reaction product by light microscopy. Within aldehyde-fixed sections incubated with a 1:100 dilution of the primary antiserum, intense immunoreactivity was detectable within small (less than

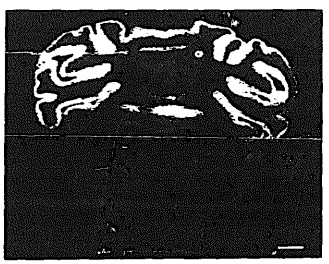

Fig. 1. Immunoautoradiographic labeling of antigenic sites in the cerebellum. The antigenic sites within sections from aldehyde-perfused rat brains were visualized using a radioactive secondary antiserum (^{125}I-IgG) and LKB Ultrofilms. The mean relative optical densities (R.O.D.) and standard deviations shown here were obtained from the section on the left that was fixed with acrolein/paraformaldehyde and incubated with a 1:1000 dilution of the primary antiserum. Since the photomicrograph of the section was produced using the LKB Ultrofilm autoradiograph as a negative, R.O.D. values are high in the white area, and low in the dark area. The R.O.D. values of PGL and WM are significantly different from that of ML ($P < 0.005$ (df = $n-1$), Student's *t*-test). Further details of the procedures are described under Materials and Methods. ML, molecular layer; PGL, Purkinje-granular layer; WM, white matter. The number of measurements taken to obtain means and standard deviations of R.O.D. are in parentheses. Bar = 100 μm.

1 μm in diameter), punctate processes and along rims of a few perikarya. Less intense, homogeneously distributed PAP reaction product was also seen throughout the section. Semi-adjacent sections incubated with the same dilution of the antiserum, but preadsorbed with the crude frog erythrocyte membrane fraction, still revealed a homogeneous distribution of the less-intense PAP reaction product, but not the intense labeling within punctate processes or perikarya. Therefore, intense immunolabeling only within the punctate processes and perikarya was considered to be specific.

Preadsorption of the antiserum at dilutions of either 1:100 or 1:1000 also completely eliminated the detectable immunoreactivity in *unfixed* cerebral cortical synaptosomal preparations as judged by either scintillation counting of the bound iodinated secondary antiserum or by quantification of the number of peroxidase-labeled postsynaptic densities (PSDs) by electron microscopy.

These observations, together with the previously reported[54] biochemical and immunocytochemical characterization of the antiserum's specificity, were used as evidence for our identification of the specific immunoreaction product as β-AR-LI. In the subsequent experiments, the methodological variables, listed below, were tested to maximize the specific-to-non-specific difference in intensity of PAP-reaction product within aldehyde-fixed sections.

Methodological variables

Dilution of primary antiserum. In either cold or room temperature incubation conditions, dilutions of the antiserum lower than 1:100 with 1- or 2-day incubations resulted in a relatively homogeneous, brown PAP-reaction product throughout the sections. In contrast, regardless of the temperature, immunoreactivity was rarely detected using dilutions of the antiserum greater than 1:4000 and incubations of up to 3 days. The most optimal labeling, as judged by the intensity of reactive profiles in contrast to the background, was seen following either: (1) a 2–3-day incubation with a 1:2000 dilution of the primary antiserum at 10 °C; or (2) a 1-day incubation with a 1:1000 dilution of the antiserum at room temperature. Under either of these conditions, light microscopic examination revealed intense immunoreactivity in punctate processes and in rims around a few perikaryal soma in both the cortex (Fig. 2A, D) and striatum (Fig. 2E).

Fixation. Using optimal dilutions of the primary antiserum and without penetration enhancing methods or amplification of the peroxidase-reaction product, immunoreactivity for the β-AR was most readily detected in tissues fixed with 4% paraformaldehyde and 0.1% glutaraldehyde at 10 °C (Fig. 2A, D and E). However, amplification of the signal through double-bridging of the PAP reaction demonstrated intense immunoreactivity in both neuronal and glial processes from brains fixed with acrolein or glutaraldehyde in combination with paraformaldehyde at room temperature (Fig. 2F, G). Except where explicitly stated, the comparisons of different dilutions of primary antiserum and permeabilizing agents as well as the quantitative ultrastructural analysis were carried out on tissues fixed under the first set of conditions and with only single-bridge PAP.

Enhancement of antisera permeability. The penetration enhancing methods employed in this study had diverse effects on the detection of peroxidase immunoreactivity under optimal dilution and fixation conditions for the primary antiserum. Firstly, the addition of 0.2% final concentration of saponin or of Triton X-100 to the incubation medium containing the primary antiserum decreased the intensity of the immunocytochemical staining, while incubation with 0.2% digitonin or the above detergents for 30 min prior to incubation with the primary antiserum resulted in a low-intensity and more diffuse reaction product (compare Fig. 2A and B). Secondly, permeabilization of membranes by rapid freeze-thawing appeared to neither increase nor decrease the detection of peroxidase immunoreactivity. Similarly the alcohol treatment was without noticeable effect on the peroxidase immunoreactivity, but did appear to reduce the presumably non-specific autoradiographic labeling of myelinated fiber bundles such as the corpus callosum.

Light and electron microscopic localization of β-AR-LI in cortex

In light microscopic examination of the cortex, the majority of the PAP-reaction product was seen in small punctate profiles. These were established by electron microscopy to include: (1) dendrites and dendritic spines; (2) small myelinated axons; (3) cel-

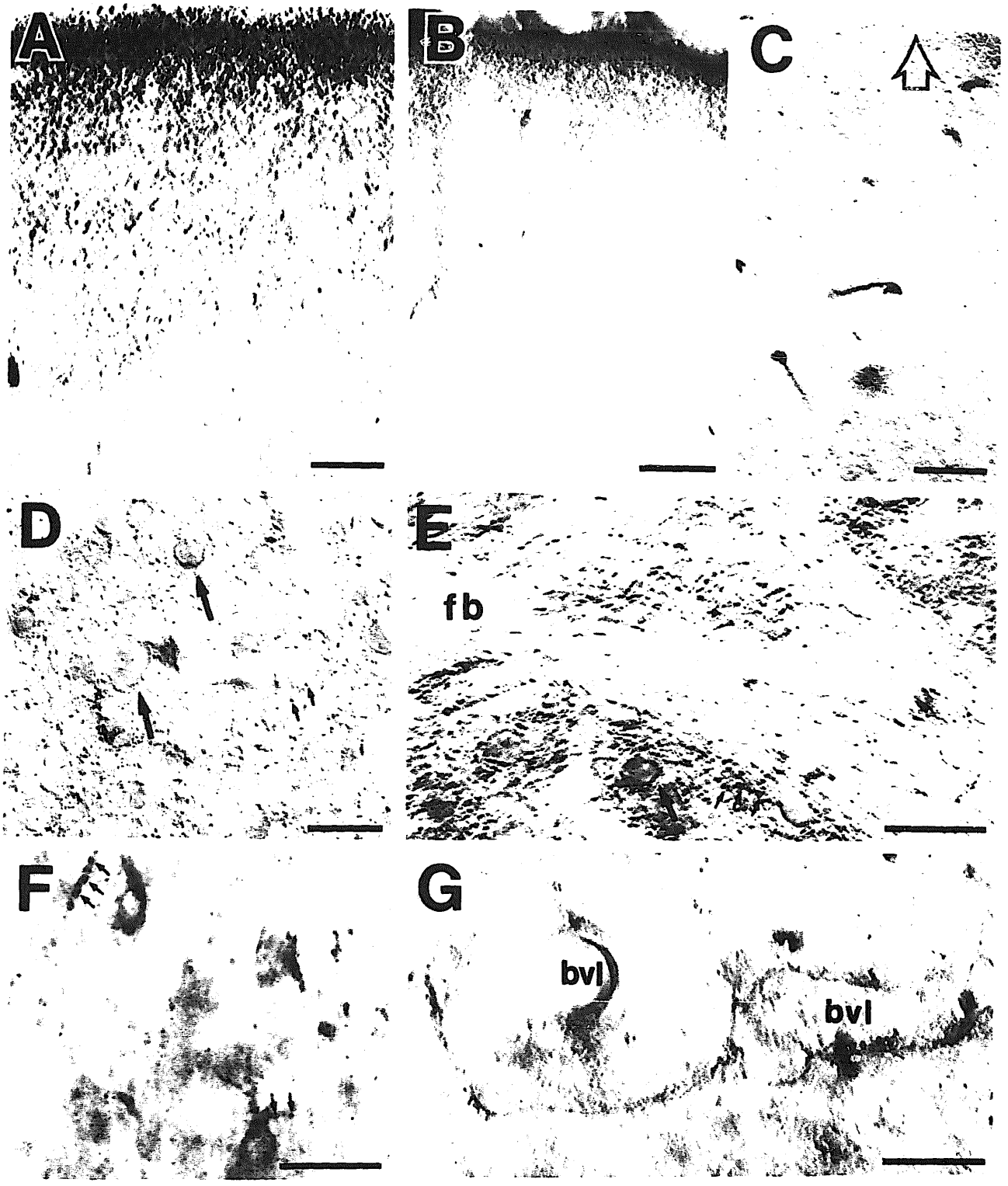

Fig. 2. Light microscopic immunocytochemistry of β-ARs. A–D, F and G, cerebral cortex (pial surface on top); E, neostriatum. A: immunocytochemical labeling of fine, punctate processes in the superficial layers of the somatosensory cortex. B: an adjacent section pretreated with digitonin for 30 min before incubation with the primary antiserum. C: an adjacent section immunoreacted with the same antiserum that had been preadsorbed by frog erythrocyte crude membrane fraction. D: the infragranular layer of the somatosensory cortex, where rims of perikarya (arrows) and numerous surrounding punctate processes (small arrows) are labeled. E: labeling of rims of perikarya (arrow) and punctate processes (small arrows) in the neostriatum. F: immunolabeling of varicosities along processes (small arrows) which may be of neurons or of glia. G: immunolabeling of fine, radiating glia-like processes along large blood vessels in the supragranular layer of the somatosensory cortex. A–E resulted from incubating paraformaldehyde/glutaraldehyde fixed sections with 1:2000 dilution of the primary antiserum for 2 days at 10 °C, while F and G resulted from incubating sections fixed in acrolein/paraformaldehyde and glutaraldehyde/paraformaldehyde, respectively, with 1:1000 dilution of the antiserum for a day at room temperature, then double-bridging. In each photomicrograph, blood vessels (clear spaces, not labeled), are visible due to differential interference contrast optics (A–E, G) or due to the osmication of tissue (F). fb, fiber bundle; bvl, blood vessel lumen. Bar = 100 μm.

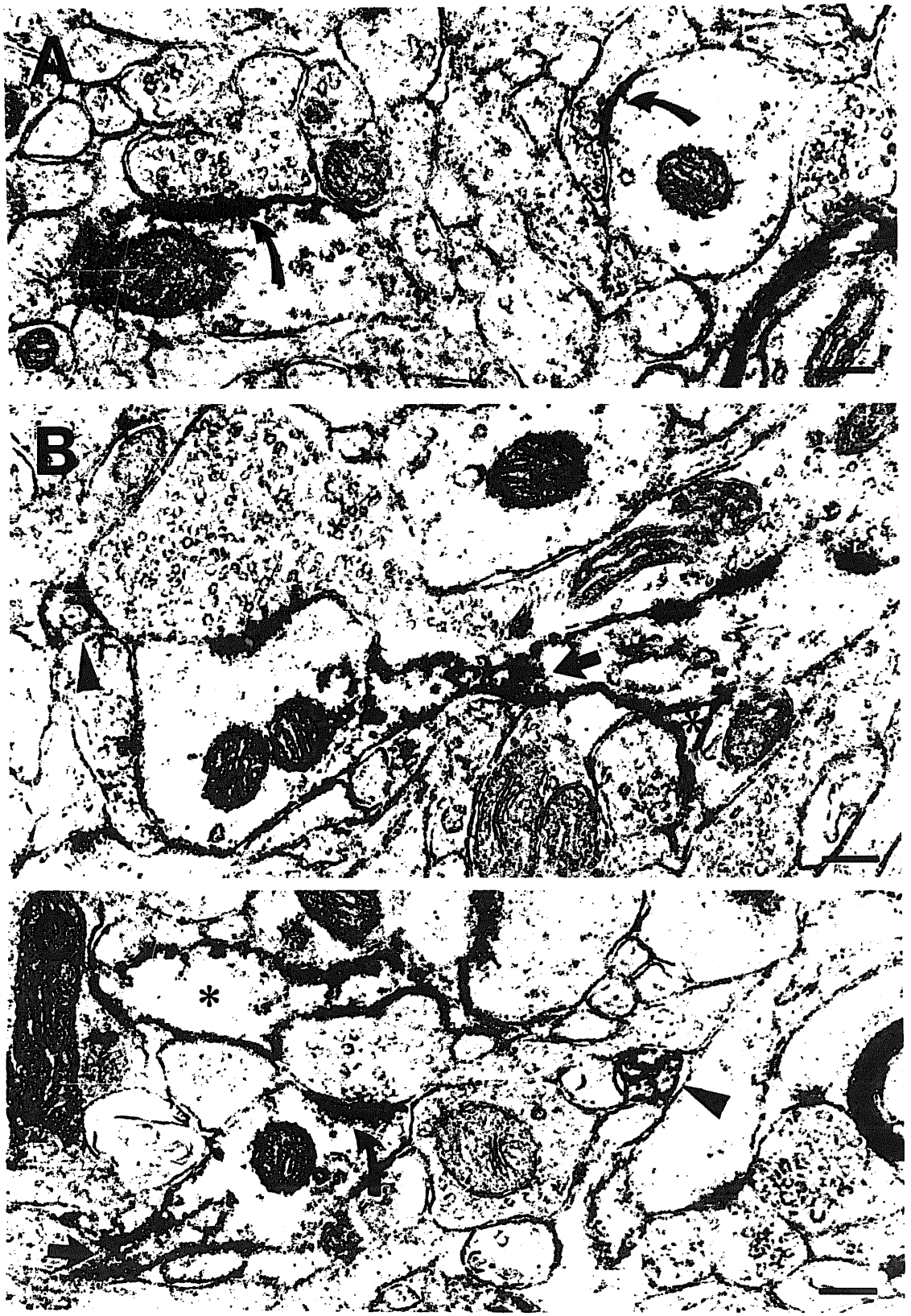

Fig. 3. Immunolabeled processes within the somatosensory cortex. A: immunolabeled thick (left arrow) and thin (right arrow) postsynaptic densities (PSDs) and the nearby mitochondria. B: accumulation of peroxidase product within the neck of a dendrite (arrow), an unidentified small process (arrowhead) and in a glia-like process (asterisk). C: immunolabeling of thick PSD (curved arrow), cytoplasmic surfaces of spine neck (straight arrow), an unidentified small process (arrowhead) and the membranes of a glia-like process (asterisk in cytoplasm). Bar = 0.2 μm.

lularly non-distinguished processes; and (4) glial-like processes.

Dendrites and dendritic spines. In aldehyde-fixed sections, the cytoplasmic surfaces of the plasmalemma and PSDs exhibited detectable immunoreactivity (Fig. 3). Frequently, the PAP product appeared to accumulate within the necks of spines (Fig. 3B, C, straight arrows) and along membranes associated with the dendritic spine apparatus (Fig. 7A, curved arrow). Other cytoplasmic elements, such as the mitochondrial outer membrane (Fig. 3A) were also usually labeled. Immunoreactivity was never detected in axons presynaptic to the labeled dendrites.

In a quantitative evaluation of the most superficial regions (Epon–tissue interface) from optimally labeled, fixed sections through the somatosensory and anterior cingulate cortical areas, 13% of the total labeled processes were associated with the cytoplasmic surfaces of dendritic processes containing PSDs (Table I). The labeled PSDs were both of asymmetric (Fig. 3A, left; B and C) and symmetric (Fig. 3A, right) synapses. Within the somatosensory cortex, these accounted for 4% (54 out of 1322) of all recognized synaptic junctions. Most labeled PSDs occurred within dendritic spines found on small (0.1–0.2 μm), distal dendrites.

Prominent localization of immunoreactivity to PSDs in the cortex, as seen in fixed sections, was also found in unfixed synaptosomal preparations. The PAP-reaction product was detected either in isolated clumps or accumulated along PSDs within the synaptosomal preparations (Fig. 4, solid arrow). Postsynaptic membranes could be distinguished from non-synaptically associated membrane fragments by the presence of an evenly-spaced intercleft zone between the postsynaptic membrane and presynaptic bouton (Fig. 4). Using a 6-h incubation at room temperature and dilutions of the primary antiserum at 1:50, 1:300 or 1:1000, immunoreactivity was assessed by quantitative electron microscopic analysis to respectively label 58 out of 160 (36%), 14 out of 121 (12%) or 14 out of 126 (12%) of the identifiable PSDs in one cortical synaptosomal preparation. In a second set of experiments, incubations for the same duration and temperature at dilutions of 1:100 and 1:1000 yielded similar frequencies of labeled PSDs. These were 15 out of 111 and 16 out of 140 identifiable synapses, respectively.

TABLE I

The distribution of labeled processes

The immunolabeled processes were identified from all of the laminae of the somatosensory and anterior cingulate areas of the cortex, as described in Materials and Methods. PSDs, dendritic profiles exhibiting identifiable postsynaptic densities; processes whose minimal diameters were less then 0.2 μm were designated as such. Adjacent processes appeared adjacent to one another within the plane of section.

Items	*Somatosensory cortex*	*Anterior cingulate cortex*
Area examined	57,143 μm^2	34,207 μm^2
Total	532 (100%)	671 (100%)
PSDs	67 (12.5%)	87 (13%)
Myelinated axons	12 (2%)	14 (2%)
<0.2 μm diameter processes	241 (45%)	274 (41%)
Adjacent processes	216 (40%)	194 (29%)
Presynaptic terminals	0 (0%)	0 (0%)

Myelinated axons. Small (0.8–2.0 μm), myelinated axons constituted only 2% of the total number of processes immunolabeled in either the somatosensory or anterior cingulate cortex (Table I). In these axons, the reaction product was detected largely on the cytoplasmic surface of the plasmalemma and along what appeared to be saccules of smooth endoplasmic reticulum and vesicles (Fig. 5). Larger myelinated axons within the same sections lacked detectable immunoreactivity.

Unidentified processes. Many of the most numerous (85% of the total labeled processes) and intensely immunoreactive processes in the somatosensory and anterior cingulate cortical areas were unidentifiable with respect to their neuronal or glial origin (Table I). Forty-five percent of the total number of immunoreactive processes were recognized only by the peroxidase-reaction product and by their small size (less than 0.2 μm in cross-sectional diameter) (Fig. 3B, C, arrowhead). These labeled processes probably include both small dendrites and unmyelinated axons as well as glial processes.

Glial processes. As anticipated from light microscopic observations of multibranched cells near blood vessels which exhibited β-AR-LI (Fig. 2G), processes having the ultrastructural characteristics of astrocytes contained peroxidase labeling. These processes were distinguished by their irregular contours, sparsity of cytoplasmic organelles other than inter-

Fig. 4. Immunolabeling of PSDs within cerebral cortical synaptosomal fraction. Synaptosomal fraction prepared from fresh, canine cerebral cortex was incubated for 6 h with 1:1000 dilution of the antiserum, then processed for PAP immunocytochemistry and electron microscopy as described under Materials and Methods. Solid arrow, immunolabeled PSD; open arrow, unlabeled PSD. Bar = 0.2 μm.

mediate filaments, and absence of any synaptic specialization along their cytoplasmic membranes (asterisk in Figs. 3B, C and 7A). Immunoreactivity within these glia-like processes was often found im-

Fig. 5. Immunolabeled myelinated axon in the somatosensory cortex. Note the accumulation of peroxidase product along a cytoplasmic membranous inclusion (solid arrow) within a labeled axon. The nearby, more heavily myelinated axons are unlabeled (open arrows). Bar = 0.2 μm.

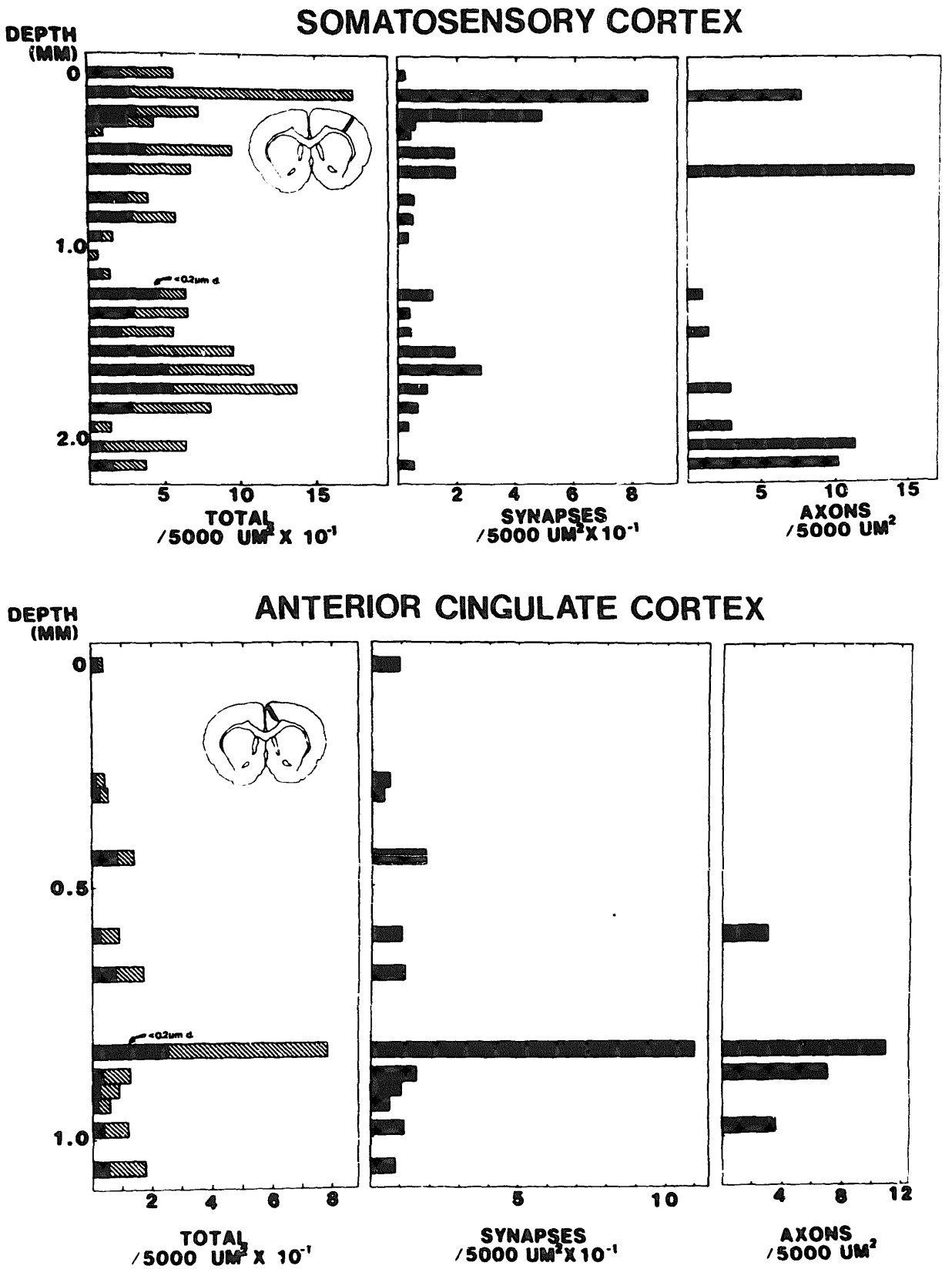

Fig. 6. Laminar distributions of labeled processes within the cerebral cortex. Serially collected ultrathin sections from flat-embedded vibratome sections that were trimmed to contain the portion indicated by the drawing (blackened within somatosensory and anterior cingulate cortical areas) were sampled for the quantitative ultrastructural analyses. For details, see Materials and Methods. Left panels: the laminar positions of immunolabeled processes of all types. Middle panels: the laminar distribution of the labeled processes that contained labeled or unlabeled PSDs. Right panels: the laminar distribution of labeled myelinated axons.

mediately adjacent to or in close proximity to another labeled process (Fig. 3B and 7A). At least 40% of all labeled processes quantitatively examined in the somatosensory cortex and 29% in the anterior cingulate cortex were adjacently positioned (Table I). However, these included appositions between labeled glial and neuronal processes as well as between neuronal, glial and unidentified processes.

Differential laminar distribution of β-AR-LI in cortex

By light microscopy, punctate, small (0.5–1.0 μm) processes showing PAP-reaction product appeared to be unevenly distributed throughout the cortical laminae (Fig. 2A). With Nomarski optics and peroxidase labeling, further differentiation of the laminar pattern in specific regions such as the somatosensory or anterior cingulate cortical areas was difficult to assess. However, quantitative analysis of peroxidase-labeled processes by electron microscopy confirmed that the laminar distribution pattern of the labeled processes greatly differed in these two cortical areas (Fig. 6). Specifically, in the somatosensory cortex, labeled processes were found most prominently in the superficial layers and least frequently in the mid-cortical layer (Fig. 6, left panel, 'total'). This general pattern was observed also within each category of labeled processes, namely those receiving identifiable synapses (Fig. 6, middle panel), those with minimal diameters of less than 0.2 μm (Fig. 6, left panel, solid bars) and for the myelinated axons (Fig. 6, right panel). In contrast to the somatosensory cortex, quantitative examination of the laminar distribution of labeled processes in the anterior cingulate cortex revealed that most of the labeling occurred within the deeper layers (Fig. 6). However as was noted in the somatosensory area, each of the categories of labeled processes had laminar distribution patterns similar to that of the total population of processes.

Quantitative confirmation of the laminar distribution in these cortical areas was obtained from macroscopic examination of sections labeled by immunoautoradiography using LKB Ultrofilm. Computer-assisted densitometric measurements revealed a significantly distinct pattern in the somatosensory and anterior cingulate cortical areas (Table II) that paralleled the pattern seen with electron microscopy (Fig. 6).

Light and electron microscopic localization of β-AR-LI in the neostriatum

Light microscopy revealed PAP-reaction product rimming the plasmalemma of a few individual perikarya and throughout numerous small (0.5–1.0-μm diameter) processes. These immunoreaction products completely filled the striatal neuropil exclusive of bundles of myelinated axons (Fig. 2E). The peroxidase reaction within the striatum appeared to be as intense as that seen in the infragranular layers of the cortex where both the punctate processes and perikaryal rims were also labeled (Fig. 2D). Quantitative

TABLE II

The laminar distribution of antigenic sites as assessed by immunoautoradiography

The methods for measuring the relative optical densities and normalizing are described under Materials and Methods. The number of hemisections examined is given in parentheses. n.d., not determined.

Area	*Mean relative optical density*					
	Animal 1 (n = 5)	*Animal 2 (n = 5)*	*Animal 3 (n = 4)*	*Animal 4 (n = 3)*	*Animal 5 (n = 9)*	*Means ± S.D.*
Somatosensory cortex						
Supragranular	1.00	1.00	1.00	1.00	1.00	1.00
Granular	0.82 ± 0.03	0.82 ± 0.02	0.86 ± 0.02	0.91 ± 0.03	0.89 ± 0.04	0.86 ± 0.04*
Infragranular	0.96 ± 0.09	0.94 ± 0.04	1.13 ± 0.08	0.94 ± 0.04	1.00 ± 0.05	1.00 ± 0.07**
Anterior cingulate cortex						
Superior	1.03 ± 0.04	1.03 ± 0.09	0.94 ± 0.12	n.d.	0.94 ± 0.07	0.99 ± 0.05**
Deep	1.22 ± 0.09	1.08 ± 0.17	1.23 ± 0.15	n.d.	1.15 ± 0.06	1.17 ± 0.06*
Neostriatum						
Dorsolateral	0.91 ± 0.08	1.01 ± 0.22	1.10 ± 0.11	n.d.	1.09 ± 0.07	1.03 ± 0.08**
Ventromedial	0.94 ± 0.08	0.86 ± 0.09	1.20 ± 0.17	n.d.	1.09 ± 0.03	1.02 ± 0.13**

*$P < 0.005$ (df = $n-1$), Student t-test; ** not significantly different $P > 0.05$.

macroscopic densitometry of immunoautoradiographs on LKB Ultrofilms confirmed that the density of immunoreactivity in the neostriatum was equivalent to the densest labeling in the somatosensory cortex (Table II).

As suggested by the light microscopic demonstra-

Fig. 7. Immunolabeling of cytoplasmic elements reported to be involved in membrane turnover. In A, the spine apparatus, (curved arrow) and the vesicle near plasma membrane (arrowhead) in this cerebral cortical dendritic spine are immunolabeled. Similarly, in B, a neostriatal process exhibits saccules near plasma membrane (solid arrow) and an endocytotic vesicle (curled arrow) that are immunolabeled, to be contrasted with an unlabeled saccule in a nearby process (open arrow). Asterisk in A points to the cytoplasm of a glia-like process; u, unlabeled glia-like process. Bar = 0.2 μm.

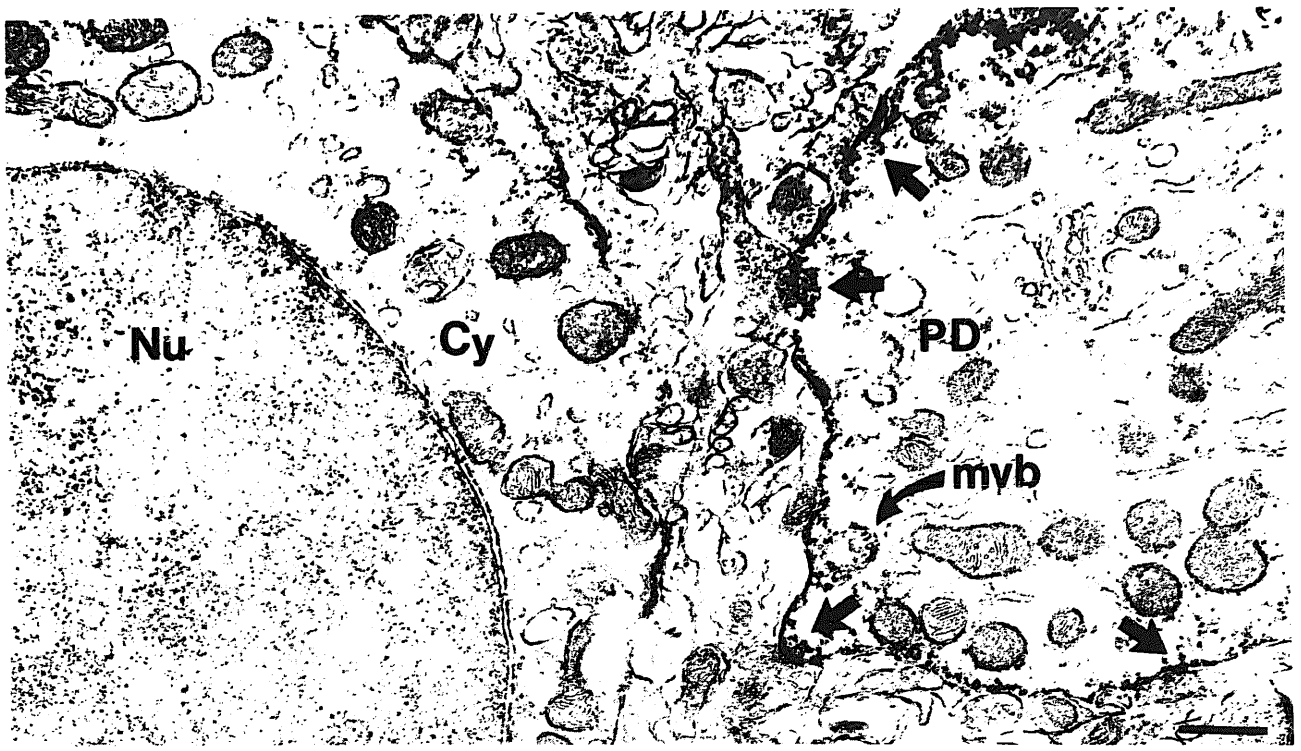

Fig. 8. Immunolabeling of the inner surface of plasmalemma of a proximal dendrite in the neostriatum. Solid arrows, immunolabeled PSDs; Nu and Cy, nucleus and cytoplasm of an unlabeled neuron; PD, immunolabeled proximal dendrite; mvb, labeled multivesicular body. Bar = 0.5 μm.

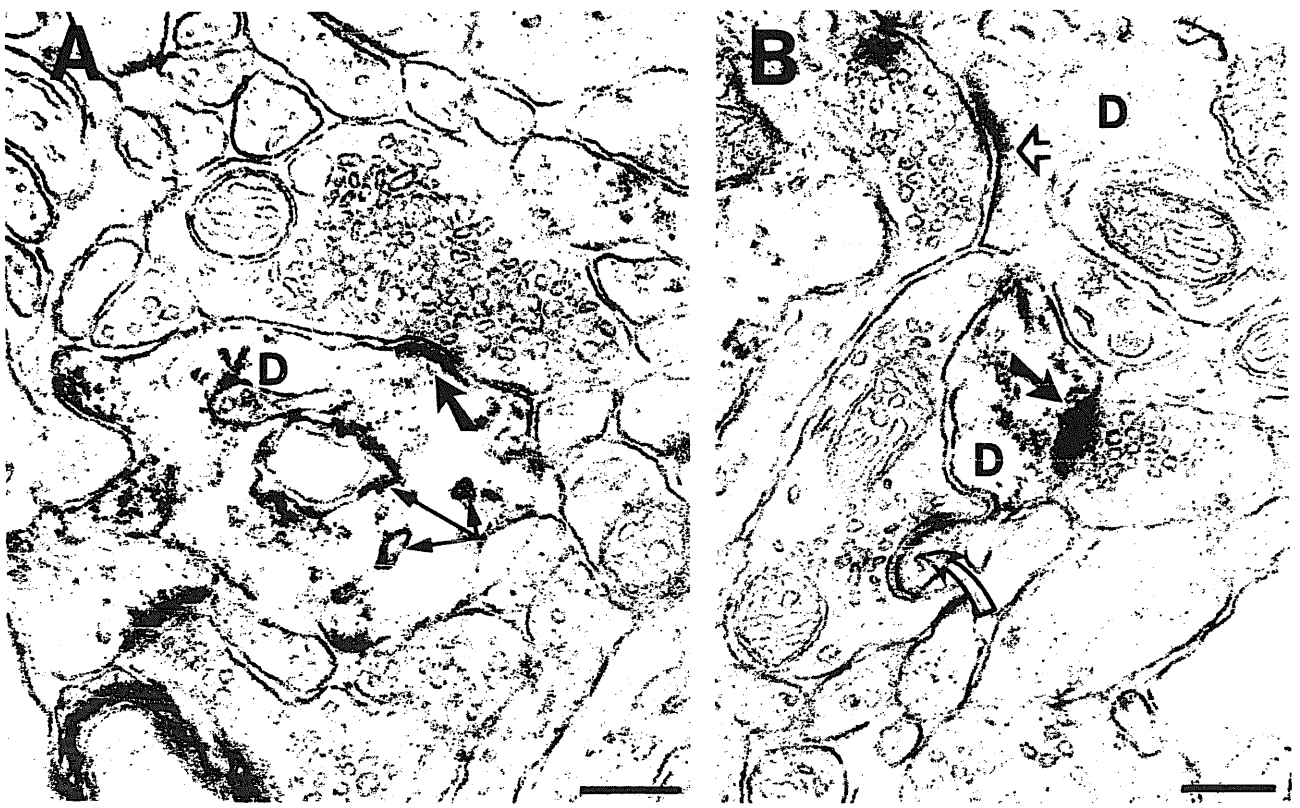

Fig. 9. Immunolabeled postsynaptic processes in the neostriatum. A: immunolabeled PSD (solid arrow) and adjacent saccules (smaller arrows). B: immunolabeled (solid arrow) and unlabeled (open arrow) PSD within a dendrite. D, dendrite. Bar = 0.2 μm.

tion of rims of PAP-reaction product near the outer boundaries of selective perikarya, accumulations of immunoreactivity also were seen along the cytoplasmic surfaces of plasmalemma of proximal dendrites examined by electron microscopy (Fig. 8). The reaction was especially evident near synapses, but was readily detected along the entire plasmalemma (Fig. 8). However, the majority of the immunoreactivity was detected in small, distal dendrites and dendritic spines (Fig. 9). Within these structures, the labeling was noted principally along the cytoplasmic surfaces of PSDs of both symmetric (Fig. 9A) and asymmetric synapses (Fig. 9B), isolated saccules of smooth endoplasmic reticulum (Fig. 7B, curved arrow) and invaginations of the plasmalemma (Fig. 7B, curled arrow). Labeled and unlabeled PSDs sometimes were seen on a common dendritic process (Fig. 9B, solid and open arrows), thus indicating that the accumulation of PAP product within the cytoplasm was satisfactorily discrete to permit the intracellular localization of the antigenic site.

DISCUSSION

Using an optimized labeling condition for immunocytochemical localization of an antiserum directed against the β-AR, we have demonstrated: (1) the applicability of quantitative electron microscopic analysis of profiles containing β-AR-LI in fixed and unfixed neural tissues; and (2) the cellular and subcellular localizations of β-AR-LI which may be of relevance to receptor-mediated events in both neurons and glia of the cerebral cortex and neostriatum.

Specificity of the antiserum

Immunoadsorption. In the present, as in the earlier[54] studies, the abolished immunoreactivity following preadsorption of the primary antiserum with a partially purified membrane preparation of the frog erythrocyte β-AR strongly suggests that the antiserum principally recognizes a protein in the fraction that is common to β-AR.

Correspondence of the immunocytochemical patterns to the known distribution of β-ARs. The immunoautoradiographic pattern of the rat cerebellum in the present study corroborates the previous light and ultrastructural localizations of immunoreactivity within the molecular layer of the cerebellum[54]. The laminar distribution of immunoreactivity within the cerebral cortex and cerebellum also resembles the previously described distribution for β-ARs, as shown by receptor autoradiography[40,46]. Further, the distribution of immunoreactivity within the anterior cingulate cortex closely reflects the noradrenergic innervation as seen with immunocytochemical labeling for the catecholamine-synthesizing enzyme, dopamine β-hydroxylase[36].

These cytochemical demonstrations of specificity are supported by the earlier biochemical studies showing that the antiserum produced: (1) immunoprecipitation of the purified β-AR; (2) alteration of the mobility of β-ARs on steric-exclusion HPLC columns; and (3) attenuation of catecholamine-sensitive adenylate cyclase[54]. Additionally, electron microscopic analyses revealed that following incubation of cortical synaptosomes with an agonist, isoproterenol, which is known to induce the internalization and subsequent translocation of β-ARs away from plasma membrane (a process called desensitization)[44,50], immunoreactivity along PSDs was abolished (unpublished observation). These evidences, taken together, suggest that the antiserum recognizes antigenic sites that are common to the β-AR. Nevertheless, it is necessary to refer to the localization as β-AR-LI, since homologies have recently been demonstrated between the β-AR and certain G protein-linked molecules, namely the hamster β_2-AR[9], the human β-AR[27], the turkey erythrocyte β-AR[58], rhodopsin[10,37] and the porcine atrial[43] and cerebral muscarinic[28] acetylcholine receptors.

Recognition of β_1- vs β_2-type receptors. The β-AR of the molecular layer of cerebellum is predominently of the β_2-type[40,46]. Thus, immunoreactivity within this area indicates that the antiserum does recognize the β_2-type adrenergic receptor. This was as expected, since the antiserum was raised by immunizing with frog erythrocytes membranes that contain β_2-ARs. However, the distributions of immunoreactivity in the cerebral cortex and the neostriatum resemble the more predominent β_1-type. These results suggest that the antiserum is not able to discriminate between the closely homologous receptor proteins[9].

Methods for optimal immunocytochemical localization of β-AR-LI

Dilution of primary antiserum. The most selective

localization of β-AR-LI is seen with dilutions of antiserum in the range of 1:1000 to 1:2000. The previous immunocytochemical study with this antiserum used at least a 10-fold higher concentration of the antiserum[54], which may have increased non-immunologic binding or even suppressed some of the specific binding to the antigen[15,18]. The higher dilutions of the present study reveal a more heterogeneous light microscopic distribution and a more specific subcellular localization of the immunoreactivity. Thus it seems likely that at least some of the peroxidase labeling in the earlier report[54] may be attributed to non-specific binding of the antiserum and/or more extensive cross-reactions with closely related proteins.

Fixation and penetration enhancing methods. When optimal dilutions of the antiserum are used, the antigenic sites qualitatively do not appear to be altered by mild fixation. The intense labeling with the β-AR-antiserum in tissues fixed with cold 4% paraformaldehyde and 0.1% glutaraldehyde is comparable to that seen for several other antigens, particularly those associated with cellular membranes[13,45]. Presumably, relatively weak fixation conditions allow penetration of the immunoglobulins to antigenic sites embedded within the plasmalemma and postsynaptic densities. This possibility is supported by our observation of intense immunoreactivity for the β-AR-LI at PSDs in *unfixed* synaptosomes with the conventional single-bridge PAP method. However, due to the amplification of the signal by double-bridging the PAP product, we also are able to detect β-AR-LI in tissues fixed with combined acrolein-and-paraformaldehyde which has been used most extensively for soluble enzymes[33] and peptides[26,32]. Failure of intra- and transmembrane fractures elicited by freeze-thawing or alcohol pretreatment to significantly enhance the detected β-AR-LI in well-fixed tissue suggests that unlike most cytoplasmic antigens, much of the receptor may be embedded among lipoproteins within the cellular membranes where they are not freely accessible with most conventional methods for enhancing penetration of antisera[12]. However, it seems likely that under the mild fixation conditions used in the present study, the receptor is not sufficiently cross-linked to the proteins of membranes to prevent extraction by digitonin, the detergent that was used to solubilize and purify β-AR from unfixed erythrocyte preparations[54].

Application of quantitative methods to ultrastructural studies for the localization of β-AR-LI

In the present study the distribution of PAP-labeled processes were quantitatively examined in fixed sections immunolabeled prior to embedding in plastic. Most earlier studies have not attempted to quantify immunoreactive processes in similarly prepared tissues largely because incomplete penetration of antisera was believed to largely invalidate the results[45]. However we have shown that laminar cortical patterns can be demonstrated by electron microscopic quantitation of the profiles showing peroxidase-reaction product, and that the pattern closely resembles that revealed by densitometry of immunoautoradiographic light microscopic localization of the β-AR-antiserum. This type of quantitation is possible only if strict criteria are applied. In particular, only those profiles in portions of the section in immediate apposition to the overlying Epon are counted. This precaution, at least partially, eliminates artifacts due to incomplete penetration. However even under these conditions, the values obtained sometimes may reflect an underestimation due either to limited penetration of the antiserum or to the difficulties of discriminating immunolabeled from electron-dense organelles. There may also be an overestimation due to failure of identifying all of the unlabeled symmetric synapses or cross-reactions of the antisera with closely related receptor subtypes. These limitations make the values obtained in this study only semiquantitative. We can, however, estimate that as many as 4–12% of the PSDs within the cortex show β-AR-LI. Considering the multiplicity of transmitter types known to exist within the cortex, this value seems high. However our results do not exclude the possibility that receptors recognizing other neurotransmitters may coexist at some or all of the sites that contain β-ARs. Conceivably, local diffusion of non-synaptically released norepinephrine[4,8,30] also may modulate the action of another synaptically released transmitter at postsynaptic sites containing the β-AR as well as other receptor types. This idea is supported by physiological evidences for the multiplicity of action of norepinephrine in regions such as the somatosensory cortex[55] and hippocampus[57]. Furthermore, norepinephrine has been shown to interact with glia[48] and with both pre- and postsynaptic sites on neurons containing GABA[2,24,56,59], serotonin[51,53], opiates[23],

acetylcholine[3] and dopamine[47]. The presently observed immunolabeling of both symmetric (Gray type II[19]) and asymmetric (Gray type I[19]) synapses also supports multiple receptive sites for norepinephrine.

The results demonstrate not only that antigens to receptor proteins can be localized in unfixed synaptosomes, but that the binding of the antiserum to the antigen can be quantitatively evaluated by peroxidase labeling and electron microscopy or by measurements of radioactivity that represents the binding of ^{125}I-secondary antiserum. The artifacts, which may be associated with alterations in antigenicity by the fixative or incomplete penetration of the antisera, are completely eliminated in the synaptosomal preparation. This preparation is much more readily manipulated with pharmacological tools and thus provides an important adjunct to ultrastructural studies of receptor localization in fixed sections of tissues.

Subcellular and cellular localization of the β-AR-LI

Regions with sparse noradrenergic innervation (neostriatum)[16] and more abundant and laminar patterns of noradrenergic innervation (cortex)[35,36] have several similarities as well as differences with respect to the localization of β-AR-LI. The densitometric measurements of immunoautoradiographs confirm the results from binding studies of the β-AR[40,46] showing that the neostriatum has a density of labeling comparable to that of the most intensely labeled cerebral cortical laminae.

In every region, the subcellular pattern of distribution of β-AR-LI appears discrete. The identity of the subcellular localization of antigens by peroxidase labeling using chromagens, such as diaminobenzidine, has been viewed with skepticism due to the cross-linking properties of glutaraldehyde and diffusion associated with the peroxidase-reaction product[38,45]. However, under optimal fixation conditions with high dilutions of the primary antiserum, a good correlation has been shown between the most intense subcellular localization as seen by electron microscopic immunocytochemistry and biochemical estimates of subcellular distribution (e.g. substance P and large granular vesicles[14,42,44]). The present observation of the coexistence of labeled and unlabeled PSDs within single dendrites further suggests that diffusion of the PAP product does not preclude a differential identification of subcellular organelles selectively labeled for the receptor. Thus, β-AR-LI is localized: (1) within PSDs, particularly in small distal dendrites; and (2) accompanying membranous structures that have been reported to be associated with endocytosis. Under optimal labeling conditions, we have also observed immunoreactivity along the intracellular surfaces of perikaryal plasmalemma. These observations suggest that the antiserum recognizes the portion of the receptor polypeptide residing in or facing the cytoplasm. These antigenic sites may reflect one or more of the hydrophilic portions of the β-AR that were recently demonstrated to be present within the cytoplasm[9,58]. Biochemical evidence also suggests that the agonist-induced desensitization of β-ARs may involve internalization of the receptors[50]. Thus the presently identified antigenic sites along membranous elements known to be involved in membrane turnover[6,41], namely the invaginations of the plasmalemma and other saccules of smooth endoplasmic reticulum within dendrites, vesicles and the spine apparatuses could reflect the internalized forms of β-ARs that are recognized by the antiserum. Furthermore the presence of antigenic sites on mitochondrial surfaces may reflect the localization of receptors which could facilitate the intracellular transport of norepinephrine for degradative oxidation by mitochondria. Alternatively, the mitochondrial localization of immunoreactivity may be due to non-specific accumulations of the reaction product, since similar reactions have been reported with many soluble enzymes[45].

The present localization of a β-AR-LI to a few myelinated axons is consistent with axonal transport and a presynaptic localization of the receptor[47]. There may be additional β-AR-LI in unmyelinated axons which remain unidentified due to difficulty in differentiating these axons from the necks of spines and small glial processes. However, the total absence of detected immunoreactivity in terminals in both the neostriatum and the cerebral cortex suggests either that the receptor protein found in terminals shows less immunoreactivity or is packaged in a form which is not accessible to the antiserum under the present labeling conditions.

The localization of β-AR-LI within glia confirms earlier reports of the presence of β-AR-specific ligand binding sites along astroglia in culture[5]. As observed in neurons, immunoreactivity is detected pri-

marily along intracellular surfaces. This suggests that antigenic sites within the β-AR molecule may be within similar domains for both neurons and glia. Our observation that many processes with morphological characteristics of astrocytes are unlabeled, even in the most superficial sections, supports the concept of functional heterogeneity among this cell type[5]. Considerable variability in the number of β-ARs associated with different types of astrocytes has previously been shown in vitro[5]. Our frequent detection of immunoreactivity in astrocytic processes in proximity to similarly labeled dendrites also is consistent with the concept that one of the functions of glial cells surrounding synapses is to control extracellular levels of transmitters by active uptake, as reviewed by Kimelberg[25]. Furthermore, Kimelberg and associates have shown a Na^+-dependent uptake of norepinephrine in cultures of astrocytes[25]. These in vivo and in vitro studies suggest that at least in the cortex, glia and neurons may be functionally integrated in response to released norepinephrine.

ACKNOWLEDGEMENTS

We thank Dr. Catherine D. Strader who generously provided the purified β_2-adrenergic receptors and offered helpful suggestions on the manuscript. We also thank June Chan and Bill Feig for their technical assistance, and Hillary Rettig and Nancy Marmor for their help in preparing the manuscript. We gratefully acknowledge the use of computer programs developed for Image Analysis by Dr. Lewis Tucker and the computer facilities made available by Dr. D.J. Reis, in the Laboratory of Neurobiology at Cornell University Medical College (NIH Grant 18974). This research was supported by research grants from NIH (HL18974), NIMH (MH40342) and NSF (BNS-8023914), to V.M.P., a career award to V.M.P. from NIMH (MH00078), and a postdoctoral award to C.A. from NIH (NS07782-01).

REFERENCES

1 Aoki, C., Kaufman, D. and Rainbow, T.C., The ontogeny of the laminar distribution of β-adrenergic receptors in the visual cortex of cats, normally reared and dark-reared, *Dev. Brain Res.*, 27 (1986) 109–116.
2 Bartholini, G., Interactions of dopaminergic, cholinergic, and GABA-ergic neurons: relation to extrapyramidal function, *Trends Pharmacol. Sci.*, 1 (1980) 138–140.
3 Bear, M.F. and Singer, W., Modulation of visual cortical plasticity by acetylcholine and noradrenaline, *Nature (London)*, 320 (1986) 172–176.
4 Beaudet, A. and Descarries, L., The monoamine innervation of rat cerebral cortex: synaptic and nonsynaptic axon terminals, *Neuroscience*, 3 (1978) 851–860.
5 Burgess, S.K. and McCarthy, K.D., Autoradiographic quantitation of beta-adrenergic receptors on neural cells in primary cultures. I. Pharmacological studies of ^{125}I-pindolol binding of individual astrocytic cells, *Brain Research*, 335 (1985) 1–9.
6 Chuang, D.M., Dillon-Carter, O., Spain, J.W., Laskowski, M.B., Roth, B.L. and Coscia, C.J., Detection and characterization of β-adrenergic receptors and adenylate cyclase in coated vesicles isolated from bovine brain, *J. Neurosci.*, 6 (1986) 2578–2584.
7 Cohen, R.S., Blomberg, F., Berzins, K. and Siekevitz, P., Structure of postsynaptic densities isolated from dog cerebral cortex. I. Overall morphology and protein composition, *J. Cell Biol.*, 74 (1977) 181–203.
8 Descarries, L., Watkins, K.C. and Lapierre, Y., Noradrenergic axon terminals in the cerebral cortex of rat. III. Topometric ultrastructural analysis, *Brain Research*, 133 (1977) 197–222.
9 Dixon, R.A.F., Kobilka, B.K., Strader, D.J., Benovic, J.L., Dohlman, H.G., Frielle, T., Bolanowski, M.A., Bennett, C.D., Rands, E., Diehl, R.E., Mumford, R.A., Slater, E.E., Sigal, I.S., Caron, M.G., Lefkowitz, R.J. and Strader, C.D., Cloning of the gene and cDNA for mammalian β-adrenergic receptor and homology with rhodopsin, *Nature (London)*, 321 (1986) 75–79.
10 Dixon, R.A.F., Sigal, I.S., Rands, E., Register, R.B., Candelore, M.R., Blake, A.D. and Strader, C.D., Ligand binding to the β-adrenergic receptor involves its rhodopsin-like core, *Nature (London)*, 326 (1987) 73–77.
11 Dolphin, A., Adrien, J., Hamon, M. and Bockaert, J., Identity of ^{3}H-dihydroalprenolol binding sites and β-adrenergic receptors coupled with adenylate cyclase in the central nervous system: pharmacological properties distribution and adaptive responses, *Mol. Pharmacol.*, 15 (1979) 1–15.
12 Eldred, W.D., Zucker, C., Karten, H.J. and Yazulla, S., Comparison of fixation and penetration enhancement techniques for use in ultrastructural immunocytochemistry, *J. Histochem. Cytochem.*, 31 (1983) 285–292.
13 Ellar, D.J., Nunoz, E. and Salton, M.R.D., The effects of low concentrations of glutaraldehyde on *Micrococcus lysodeikticus*: changes in the release of membrane associated enzymes and membrane structure, *Biochim. Biophys. Acta*, 255 (1970) 140–149.
14 Floor, E. and Leeman, S.E., Substance P-sulfoxide: separation from Substance P by high pressure liquid chromatography, biological and immunological activities and chemical reduction, *Anal. Biochem.*, 101 (1980) 498–503.
15 Forssmann, W.G., Pickel, V., Reinecke, M., Hock, D. and Metz, J., Immunohistochemistry and immunocytochemistry of nervous tissue. In Ch. Heym and W.-G. Forssmann (Eds.), *Techniques in Neuroanatomical Research*, Springer, New York, 1981, pp. 171–205.
16 Glowinski, J. and Iverson, L.L., Regional studies of catecholamines in rat brain, *J. Neurochem.*, 13 (1966) 655–667.

17 Goldenthal, K.L., Hedman, K., Chen, J.W., August, J.T. and Willingham, M.C., Postfixation detergent treatment for immunofluorescence suppresses localization of some integral membrane proteins, *J. Histochem. Cytochem.*, 33 (1985) 813–820.
18 Grube, D., Immunoreactivities of gastrin (G) cells. II. Non-specific binding of immunoglobulins to G-cells by ionic interactions, *Histochemistry*, 66 (1980) 149–167.
19 Gray, E.G., Axosomatic and axo-dendritic synapses of the cerebral cortex: an electron microscope study, *J. Anat.*, 93 (1959) 420–433.
20 Hamel, E. and Beaudet, A., Localization of opioid binding sites in rat brain by electron microscopic radioautography, *J. Electron Microsc. Technol.*, 1 (1984) 317–329.
21 Houser, C.R., Crawford, G.D., Barber, R.P., Salvaterra, P.M. and Vaughn, J.E., Organization and morphological characteristics of cholinergic neurons: an immunocytochemical study with a monoclonal antibody to choline acetyltransferase, *Brain Research*, 266 (1983) 97–119.
22 Iadecola, C., Nakai, M., Mraovitch, S., Ruggiero, D.A., Tucker, L.W. and Reis, D.J., Global increase in cerebral metabolism and blood flow produced by focal electrical stimulation of dorsal medullary reticular formation in rat, *Brain Research*, 272 (1983) 101–114.
23 Iwamoto, E.T. and Way, E.L., Opiate actions and catecholamines, *Ann. Biochem. Psychopharmacol.*, 20 (1979) 357–428.
24 Jahr, C.E. and Nicoll, R.A., Noradrenergic modulation of dendodendritic inhibition in the olfactory bulb, *Nature (London)*, 297 (1982) 227–229.
25 Kimelberg, H.K., Primary astrocyte cultures — a key to astrocyte function, *Cell Molec. Neurobiol.*, 3 (1983) 1–16.
26 King, J.C., Lechan, R.M., Kugel, G. and Anthony, E.L.P., Acrolein: a fixative for immunocytochemical localization of peptides in the central nervous system, *J. Histochem. Cytochem.*, 31 (1983) 62–68.
27 Kobilka, B.K., Dixon, R.A.F., Frielle, T., Dohlman, H.G., Bolanowski, M.A., Sigal, I.S., Yang-Feng, T.L., Francke, U., Caron, M.G. and Lefkowitz, R.J., cDNA for the human β_2-adrenergic receptor: a protein with multiple membrane-spanning domains and encoded by a gene whose chromosomal location is shared with that of the receptor for platelet-derived growth factor, *Proc. Natl. Acad. Sci. U.S.A.*, 83 (1987) 46–50.
28 Kubo, T., Fukuda, K., Mikami, A., Maeda, A., Takahashi, H., Mishina, M., Haga, T., Haga, K., Ichiyama, A., Kangawa, K., Kojima, M., Matsuo, H., Hirose, T. and Numa, S., Cloning, sequencing and expression of cDNA encoding the muscarinic acetylcholine receptor, *Nature (London)*, 323 (1986) 411–416.
29 Lefkowitz, R.J., Stadel, J.M. and Caron, M.G., Adenylate cyclase-coupled β-adrenergic receptors: structure and mechanisms of activation and desensitization, *Annu. Rev. Biochem.*, 52 (1983) 159–186.
30 Libet, B., Nonclassical synaptic functions of transmitters, *Fed. Proc. Fed. Am. Soc. Exp. Biol.*, 45 (1986) 2678–2686.
31 McLean, S., Skirboll, L.R. and Pert, C.B., Opiatergic projection from the bed nucleus to the habenula: a demonstration by a novel radioimmunohistochemical method, *Brain Research*, 278 (1983) 255–267.
32 Milner, T.A. and Pickel, V.M., Ultrastructural localization and afferent sources of Substance P in the rat parabrachial region, *Neuroscience*, 17 (1986) 687–707.
33 Milner, T.A., Joh, T.H. and Pickel, V.M., Tyrosine hydroxylase in the rat parabrachial region: ultrastructural localization and extrinsic sources of immunoreactivity, *J. Neurosci.*, 6 (1986) 2585–2603.
34 Minneman, K.P., Hegstrand, L.R. and Molinoff, P.B., Simultaneous determination of beta-1 and beta-2 adrenergic receptors in tissue containing both receptor subtypes, *Molec. Pharmacol.*, 16 (1979) 34–36.
35 Morrison, J.H., Grzanna, R., Molliver, M.E. and Coyle, J.T., The distribution and orientation of noradrenergic fibers in neocortex of rat: an immunofluorescence study, *J. Comp. Neurol.*, 181 (1978) 17–40.
36 Morrison, J.H., Molliver, M.E., Grzanna, R. and Coyle, J.T., Noradrenergic innervation patterns in three regions of medial cortex: an immunofluorescence characterization, *Brain Res. Bull.*, 4 (1979) 849–857.
37 Nathans, J. and Hogness, D.S., Isolation, sequence analysis, and intron-exon arrangement of the gene encoding bovine rhodopsin, *Cell*, 34 (1983) 807–814.
38 Novikoff, A.B., Novikoff, P.M., Quintana, N. and Davis, C., Diffusion artifacts in 3,3'-diaminobenzidine cytochemistry, *J. Histochem. Cytochem.*, 20 (1972) 745.
39 Ordronneau, P., Lindström, P.B.-M. and Petrusz, P., Four unlabeled antibody bridge techniques: a comparison, *J. Histochem. Cytochem.*, 29 (1981) 1397–1404.
40 Palacios, J.M. and Kuhar, M.J., Beta-adrenergic receptor localization by light microscopic autoradiography, *Science*, 208 (1980) 1378–1380.
41 Pastan, I. and Willingham, M.C. (Eds.), *Endocytosis*, Plenum, New York, 1985.
42 Pelletier, G., Steinbusch, H.W.M. and Verhofstad, A.A.J., Immunoreactive substance P and serotonin present in the same dense-core vesicles, *Nature (London)*, 293 (1981) 71–72.
43 Peralta, E.G., Winslow, J.W., Peterson, G.L., Smith, D.H., Ahskenazi, A., Ramachandran, J., Schimerlik, M.I. and Capon, D.J., Primary structure and biochemical properties of an M_2 muscarinic receptor, *Science*, 236 (1987) 600–605.
44 Pickel, V.M., Reis, D.J. and Leeman, S.E., Ultrastructural localization of substance P in neurons of rat spinal cord, *Brain Research*, 122 (1977) 534–540.
45 Pickel, V.M., Immunocytochemical Methods. In L. Heimer and M.J. Robards (Eds.), *Neuroanatomical Tract-Tracing Methods*, Plenum, New York, 1981.
46 Rainbow, T.C., Parsons, B. and Wolfe, B.B., Quantitative autoradiography of $beta_1$- and $beta_2$-adrenergic receptors in rat brain, *Proc. Natl. Acad. Sci. U.S.A.*, 81 (1984) 1585–1589.
47 Reisine, T.D., Chesselet, M.F., Lutebzki, C., Cheramy, A. and Glowinski, J., The role for striatal β-adrenergic receptors in the regulation of dopamine release, *Brain Research*, 241 (1982) 123–130.
48 Rougon, G., Noble, M. and Mudge, A.W., Neuropeptides modulate the beta-adrenergic response of purified astrocytes in vitro, *Nature (London)*, 305 (1983) 715–717.
49 Schachner, M., Hedley-Whyte, E.T., Hsu, D.W., Schoonmaker, G. and Bignami, A., Ultrastructural localization of glial fibrillary acidic protein in mouse cerebellum by immunoperoxidase, *J. Cell Biol.*, 75 (1977) 67.
50 Sibley, D.R. and Lefkowitz, R.J., Molecular mechanisms of receptor desensitization using a β-adrenergic receptor-coupled adenylate cyclase system as a model, *Nature (London)*, 317 (1985) 124–129.
51 Snyder, A.M., Zigmond, M.J. and Lung, R.D., Sprouting

of serotonergic afferents into striatum after dopamine-depleting lesions in infant rats: a retrograde transport and immunocytochemical study, *J. Comp. Neurol.*, 245 (1986) 274–281.

52 Sternberger, L.A., *Immunocytochemistry*, Wiley and Sons, New York, 1979.

53 Stockmeier, C.A., Martino, A.M. and Kellar, K.J., A strong influence of serotonin axons on β-adrenergic receptors in rat brain, *Science*, 230 (1985) 323–325.

54 Strader, C.D., Pickel, V.M., Joh, T.H., Strohsacker, M.W., Shorr, R.G.L., Lefkowitz, R.J. and Chron, M.C., Antibodies to the β-adrenergic receptor: attenuation of catecholamine-sensitive adenylate cyclase and demonstration of postsynaptic receptor localization in brain, *Proc. Natl. Acad. Sci. U.S.A.*, 80 (1983) 1840–1844.

55 Waterhouse, B.D. and Woodward, D.J., Interaction of norepinephrine and cerebrocortical activity evoked by stimulation of somatosensory afferent pathways in the rat, *Exp. Neurol.*, 67 (1980) 11–34.

56 Waterhouse, B.D., Moises, H.C., Yeh, H.H. and Woodward, D.J., Norepinephrine enhancement of inhibitory synaptic mechanisms in cerebellum and cerebral cortex: mediation by β-adrenergic receptors, *J. Pharmacol. Exp. Ther.*, 221 (1982) 495–506.

57 Winson, J. and Dahl, D., Action of norepinephrine in the dentate gyrus. II. Iontophoretic studies, *Exp. Brain Res.*, 59 (1985) 497–506.

58 Yarden, Y., Rodriguez, H., Wong, S.K.-F., Brandt, D.R., May, D.C., Burnier, J., Harkins, R.N., Chen, E.Y., Ramachandran, J., Ullrich, A. and Ross, E.M., The avian β-adrenergic receptor: primary structure and membrane topology, *Proc. Natl. Acad. Sci. U.S.A.*, 83 (1986) 6795–6799.

59 Yeh, H.H. and Woodward, D.J., Beta-1 adrenergic receptors mediate noradrenergic facilitation of Purkinje cell response to GABA in cerebellum of rat, *Neuropharmacology*, 22 (1983) 629–639.